

CHEMISTRY

A European Journal

A Journal of



Accepted Article

Title: Hydroxylated fluorescent dyes for live cell labeling: synthesis, spectra and superresolution STED** microscopy

Authors: Vladimir N Belov, Alexey N Butkevich, Kirill Kolmakov, Viktor V Sokolov, Heydar Shojaei, Sven C Sidenstein, Dirk Kamin, Jessica Matthias, Rifka Vlijm, Johann Engelhardt, and Stefan W Hell

This manuscript has been accepted after peer review and appears as an Accepted Article online prior to editing, proofing, and formal publication of the final Version of Record (VoR). This work is currently citable by using the Digital Object Identifier (DOI) given below. The VoR will be published online in Early View as soon as possible and may be different to this Accepted Article as a result of editing. Readers should obtain the VoR from the journal website shown below when it is published to ensure accuracy of information. The authors are responsible for the content of this Accepted Article.

To be cited as: *Chem. Eur. J.* 10.1002/chem.201701216

Link to VoR: <http://dx.doi.org/10.1002/chem.201701216>

Supported by
ACES

WILEY-VCH

Hydroxylated fluorescent dyes for live cell labeling: synthesis, spectra and superresolution STED** microscopy

Alexey N. Butkevich,* Vladimir N. Belov,* Kirill Kolmakov, Viktor V. Sokolov, Heydar Shojaei, Sven C. Sidenstein, Dirk Kamin, Jessica Matthias, Rifka Vlijm, Johann Engelhardt and Stefan W. Hell*

Abstract: Hydroxylated rhodamines, carbopyronines, silico- and germanorhodamines with absorption maxima in the range of 530–640 nm were prepared and applied in specific labeling of living cells. The direct and high-yielding entry to germa- and silaxanthenones tolerates the presence of protected heteroatoms and may be considered for the syntheses of various sila- and germafluoresceins, as well as -rhodols. Application in stimulated emission depletion (STED) fluorescence microscopy revealed a resolution of 50–75 nm in one- and two-color imaging of vimentin-HaloTag fused protein and native tubulin. The established structure-property relationships allow prediction of the spectral properties and the positions of spiro-lactone/zwitterion equilibria for the new analogs of rhodamines, carbo-, silico- and germanorhodamines using simple additive schemes.

Among the multitude of fluorophores reported so far, only rhodamines,^[1] carbopyronines,^[1a] and silicon-rhodamines (SiR)^[2] bearing a carboxyl in the *ortho*-position of the pendant aromatic ring provide specific vital labeling and perform well in superresolution fluorescence microscopy. These dyes exist in equilibrium between zwitterionic (fluorescent) and spiro-lactone (non-fluorescent) forms. Many cationic lipophilic triarylmethanes bind non-specifically and stain membrane structures.^[3] Numerous anionic fluorescent labels, commercially available as sulfonates or phosphates, are hydrophilic and highly water-soluble but do not penetrate the plasma membrane and are therefore used nearly exclusively in immunostaining of fixed cells; alternative strategies of membrane-impermeant label delivery employ cell-penetrating peptide conjugates^[4] and reversible permeabilization.^[5] On the contrary, several rhodamine-type dyes specifically stain intact cells when applied as conjugates with small molecule recognition units.^[1a, 2a, 2c, 6] The most widely used recognition units are BG-NH₂, BC-NH₂ and HaloTag amine

(covalent ligands of the SNAP-tag,^[7] CLIP-tag,^[8] and HaloTag proteins^[9]). Several non-covalent ligands (such as docetaxel, jasplakinolide, or pepstatin A binding to native β -tubulin,^[2b] F-actin^[2b] or aspartyl proteases in lysosomes,^[2c] respectively) have been successfully used as conjugates with fluorescent dyes (see Figure S1, *Supporting Information*). However, the affinity and staining specificity of a given marker depends on the cell line, the nature of the ligand and the dye, the length of the linker between them and the cell staining buffer composition.^[2b] Moreover, the spectral variety of photostable dyes suitable for live cell superresolution microscopy still remains limited.

To address some of the above-stated limitations, we have recently proposed the introduction of hydroxyl groups into the fluorescent dye molecules as a method for increasing polarity, improving solubility in water and preventing unspecific binding. In our previous study, we reported the dye 580R^[1a, 10] (a live-cell two-color STED imaging marker), a rhodamine with two hydroxyl groups in allylic positions. In 580R and its predecessor Atto 590,^[1b] the conjugated alkene bonds in dihydroquinoline fragments provide the bathochromic and bathofluoric shifts.^[1a, 10] However, these fragments are prone to photooxidation and may negatively affect the photostability.^[11] Aimed at developing methods for preventing unspecific binding and improving water solubility of fluorescent dyes for living cells, we have designed fluorophores with additional hydroxyl groups (530RH and 575RH, Figure 1) in non-allylic and non-benzylic positions.

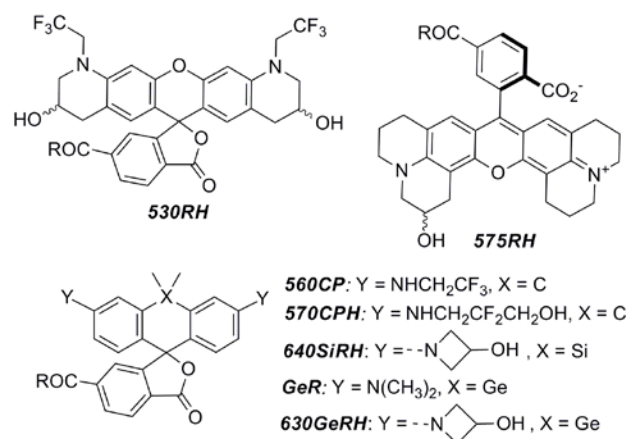


Figure 1. Membrane-permeant and fluorescent rhodamines (R), carbopyronines (CP), silicon- (SiR) or germano-rhodamines (GeR) designed for STED microscopy of living cells (in free dyes, R = OH; in dye-ligand conjugates, R = NH-ligand or NH-linker-ligand). H in names stands for hydroxylated fluorophores.

[*] Dr. A. N. Butkevich, Dr. V. N. Belov, Dr. K. Kolmakov, Dr. H. Shojaei, Dr. S. C. Sidenstein, Dr. D. Kamin, Prof. Dr. Dr. h. c. S. W. Hell, Department of Nanobiophotonics, Max Planck Institute for Biophysical Chemistry (MPIBPC), Am Fassberg 11, 37077 Göttingen, Germany
E-mail: abutkev@gwdg.de, vbelov@gwdg.de, shell@gwdg.de
Website: <http://www.mpiibpc.gwdg.de/abteilungen/200/>
Dr. V. V. Sokolov, Department of Chemistry, St. Petersburg State University, Universitetskij Pr. 26, 198504 St. Petersburg, Russia
MSc J. Matthias, Dr. R. Vlijm, Dr. J. Engelhardt, German Cancer Research Center (DKFZ), Im Neuenheimer Feld 280, 69120 Heidelberg, Germany

[**] STED: stimulated emission depletion

Supporting information for this article is given via a link at the end of the article.

Table 1. Spectral properties of cell-permeant dyes in aqueous PBS buffer (pH 7.4) at room temperature (STED at 775 nm, unless noted otherwise).

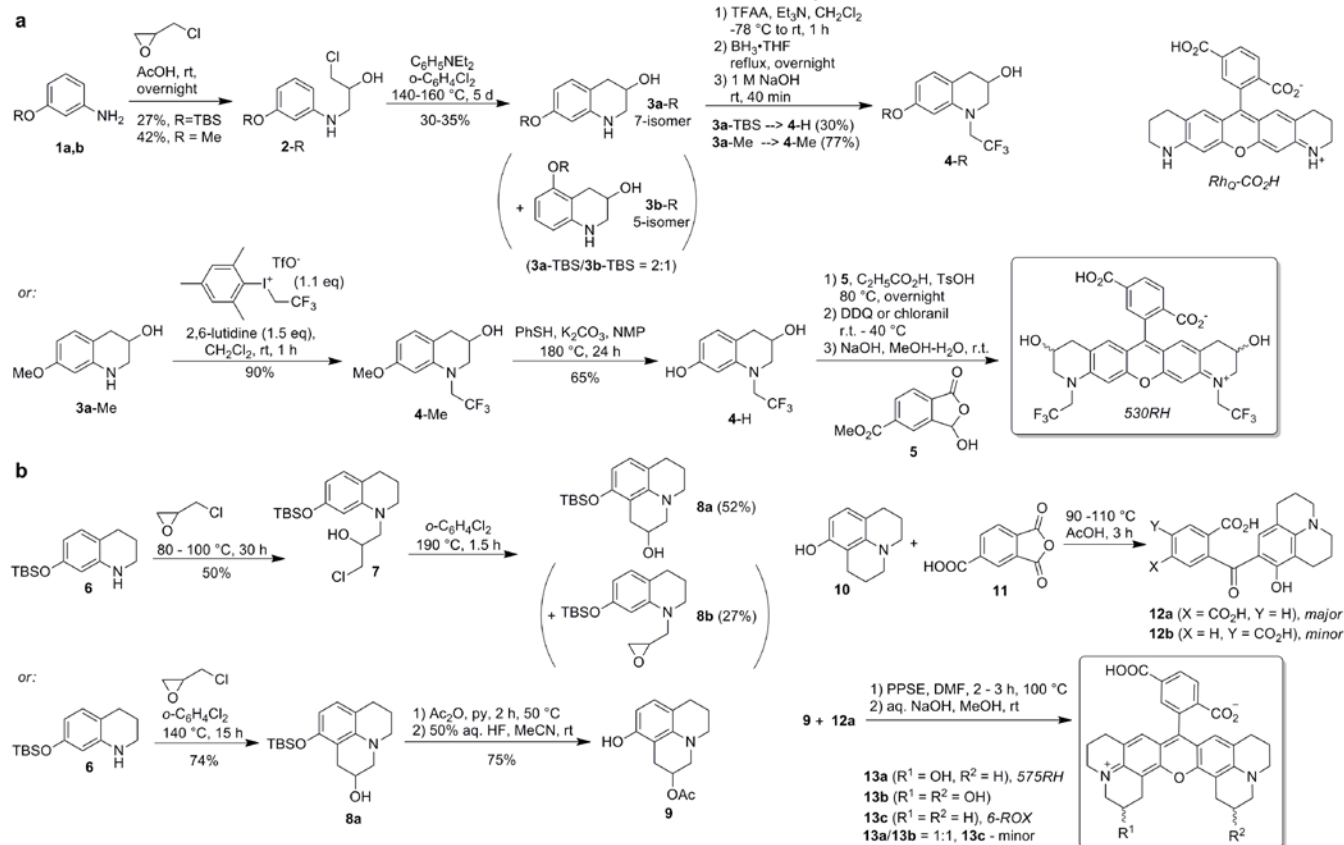
Dye	Absorption λ_{max} , nm (ϵ , $\text{M}^{-1} \text{cm}^{-1}$)	Emission λ_{max} , nm (Φ_{fl}) ^[a]	Brightness rel. to SiR ^[b]	$D_{0.5}$ ^[c]	Fluor. lifetime τ , ns
<i>Rh_QCO₂H</i> ^[1d]	540 (70000)	561 (0.79)	1.45	<5.6	4.0
<i>530RH</i>	532 (56000)	553 (0.89) ^[d,e]	1.31	29.6	4.0
<i>560CP</i>	561 (61000)	588 (0.76) ^[e]	1.22	71.0	4.2
<i>570CPH</i>	571 (79000)	600 (0.71)	1.47	58.5	4.0
<i>6-ROX</i> ^[f]	575 (82000)	602 (0.76)	1.63	<5.6	4.3
<i>575RH</i>	574 (55000)	597 (0.74)	1.07	<5.6	4.3
<i>GeR</i>	634 (97000)	655 (0.43)	1.09	65.2	2.7
<i>630GeRH</i>	631 (61000)	651 (0.60)	0.96	72.2	3.2
<i>SiR</i> ^[2]	645 (93000)	661 (0.41)	1 (ref.)	64.5	2.7
<i>640SiRH</i>	641 (51000)	662 (0.42)	0.56	72.4	3.2

H denotes hydroxylated fluorophores. [a] absolute values; [b] relative brightness expressed as $(\epsilon \times \Phi_{\text{fl}})_{\text{dye}} / (\epsilon \times \Phi_{\text{fl}})_{\text{SiR}}$; [c] see ref.[1a] for the definition of $D_{0.5}$; [d] pulsed STED at 631 nm; [e] CW gated STED at 660 nm (LEICA microsystems); [f] 6'-COOH-X-Rhodamine.

Substitution of an oxygen atom in pyronines with a 14 group element atom ($X = \text{Si}, \text{Ge}, \text{Sn}$) leads to significant bathochromic and bathofluoric shifts.^[2,12] The effect is due to lower LUMO energy of these fluorophores explained by

conjugation between the σ^* orbitals of exocyclic X–R bonds and the π^* -system of the X-containing tricyclic fragment.^[12] The extent of the red shift falls in the order $\text{Si} > \text{Ge} > \text{Sn}$ ($>> \text{C}$), as the efficiency of $\sigma^*-\pi^*$ overlap decreases with the increasing atomic radius of X and C–X bond length. The corresponding Sn-pyronine dyes are unstable; however, *GeR* dye, the direct Ge analog of the widely used fluorogenic dye *SiR*,^[2a] and its bis-azetidyl analog (Ge analog of the dye *JF₆₄₆*)^[6] remain unknown^[13] (Figure S2). To investigate the properties of the new fluorophores and the influence of hydroxylation on staining specificity, we prepared dyes listed in Table 1 (see also Figure S3).

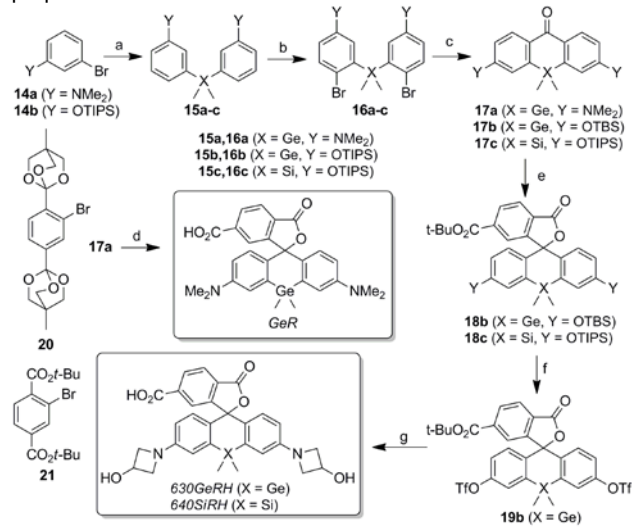
Bis-hydroxylated dye *530RH* with 6'-carboxy-Q-rhodamine (*Rh_Q-CO₂H*)^[14] core was prepared according to Scheme 1, a. While the parent *Rh_Q-CO₂H* is cell-permeant and its conjugate with HaloTag amine provided specific staining in living cells,^[1d] the dye is poorly soluble in aqueous media and its secondary amino groups are prone to acylation, rendering its NHS ester unstable. To get rid of these drawbacks, a new dye *530RH*, having two 2,2,2-trifluoroethyl groups to block its nitrogen atoms from acylation and two hydroxyl groups to offset the hydrophobic properties of *N*-trifluoroethyl substituents, was designed. These substituents impart only slight bathochromic and bathofluoric shifts but shift the equilibrium between zwitterionic and spiroactone forms significantly towards the latter,^[1a] facilitating cell membrane penetration. Following the same logic, the dye *560CP* (Figure S4) and its hydroxylated analog *570CPH* were designed as useful derivatives of the *N,N'*-unsubstituted carbopyronine, which itself has not yet found any application in fluorescent labeling.



Scheme 1. a) Synthesis of the bis-hydroxylated rhodamine dye *530RH* (an analog of *Rh_Q-CO₂H*). b) Synthesis of hydroxylated ROX dyes (6-COOH-X-Rhodamines) *575RH* (**13a**) and **13b**. Alternative schemes indicate better yielding sequences. PPSE = trimethylsilyl polyphosphate.

The synthesis of hydroxylated ROX dyes – 6'-carboxy-derivatives of *X*-rhodamine (Rhodamine 101), known to have high fluorescence quantum yields both in organic and aqueous solutions – is shown in Scheme 1, b. The scrambling condensation between acetate **9** and benzophenone **12a** afforded two other dyes (**13b,c**) besides the expected **575RH** (**13a**) due to two consecutive acid-catalyzed reactions: retro-Friedel-Crafts dissociation of **12a** to compounds **10** and **11** (or trimellitic acid), followed by Friedel-Crafts acylation of **9** with **11**. As a result, a new benzophenone with 2-hydroxy- or 2-acetoxyjulolidine fragment was formed, leading to dihydroxylated dye **13b**. 6-ROX (**13c**) arose similarly from the retro-Friedel-Crafts byproduct **10**.

The hydroxylated analogs of the unknown bis-(*N*-azetidiny)-*GeR* and *JF*₆₄₆^[6] – dyes **630GeRH** and **640SiRH**, respectively – were prepared following the general route on Scheme 2. The method involves a regioselective bromination of di-*O*-TIPS-protected bis(3-hydroxyphenyl)silanes or -germanes **16b,c** (TIPS group is required for selectivity) and a double lithium-halogen exchange on dibromides **16** followed by a reaction with dimethylcarbamoyl chloride to yield germa- and silaxanthenes **17**. The intermediates **17** are general precursors to the variety of sila- and germafluoresceins and -rhodols, and the proposed approach offers a significant improvement with regard to the number of steps,^[6, 15] yield^[16] and functional group tolerance as compared to earlier preparations.



Scheme 2. Synthesis of *GeR* and *SiR* dyes. a) *n*-BuLi, -78 °C, then Me₂GeCl₂ or Me₂SiCl₂; b) NBS; c) *n*-BuLi or *tert*-BuLi, -78 °C, then Me₂NCOCl; d) **20**, *tert*-BuLi (2 eq), -78 °C to rt, then 6 M HCl, 80 °C; e) **21**, *n*-BuLi, THF-pentane, -100 °C to rt; f) TBAF, then Tf₂O, pyridine; g) 3-(*tert*-butylsilyloxy)azetidone, Pd₂(dba)₃, XPhos, K₂CO₃ (3 eq), dioxane, 100 °C, then TBAF, then TFA, CH₂Cl₂.

To evaluate the response of our dyes to the polarity of the media, a series of absorption spectra were recorded in aqueous dioxane solutions with varying water content. The spiro-lactone-zwitterion equilibrium is shifted in favor of the colored and fluorescent zwitterionic form as the water content increases (Figure 2). For each dye, the $D_{0.5}$ parameter,^[1a] an interpolated dielectric constant of the dioxane-water mixture at which the normalized absorption A/A_{\max} (or extinction ϵ/ϵ_{\max}) of this dye equals one half of the maximal value observed across the entire dioxane-water gradient, was determined (Table 1).

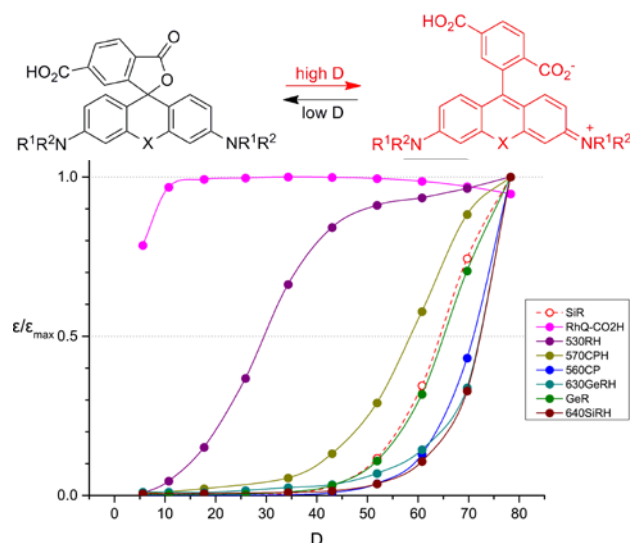


Figure 2. Normalized extinction ϵ/ϵ_{\max} at λ_{\max} of the dyes from Table 1 versus dielectric constant D of dioxane-water mixtures (**575RH** and **6-ROX** are unresponsive and are not included). The $D_{0.5}$ values correspond to the intersection of interpolated graphs with $\epsilon/\epsilon_{\max} = 0.5$ line.^[1a]

As expected, the colorless spiro-lactones of *GeR*, fluorinated rhodamine **530RH** and carbopyronine **560CP** undergo ring opening to the colored and fluorescent zwitterionic forms in systems with high water content, while electron-rich ROX derivatives remain unresponsive, existing predominantly in the zwitterionic form (Figure S5). Hydroxylation of the *N*-alkyl substituents shifts the position of the equilibrium towards the spiro-lactone form as can be expected from the weak $-I$ effect of β -hydroxy substituents (the increase in $D_{0.5}$ observed upon transition from *SiR* to **640SiRH** and from *GeR* to **630GeRH** is 7-8 units). The hydroxylated dyes appear photophysically very similar to the parent fluorophores, demonstrating up to 0.5 ns longer fluorescence lifetimes and, in the case of **630GeRH**, an improved fluorescence quantum yield.

In agreement with our earlier observations,^[1a] HaloTag(O2) amine ligands derived from silico- and germanorhodamines, as well as from fluorinated carbopyronines **560CP** and **570CPH**, demonstrated significant fluorogenic response (increase in fluorescence intensity upon covalent binding to HaloTag protein) in the presence of serum proteins background (Figure S6). The magnitude of the response was consistently smaller for hydroxylated dyes, suggesting a decreased binding affinity of hydroxylated ligands. We can therefore conclude that moderate or high values of $D_{0.5}$ seem to be required, but not sufficient for the desirable fluorogenic behavior of triarylmethane fluorescent labels^[1a, 2c].

For the evaluation of performance of our new dyes in superresolution microscopy, living HeLa and U2OS cells expressing a vimentin-HaloTag fusion protein were incubated for 20 min with 1 μ M solutions of **530RH**, **570CPH**, **575RH**, **630GeRH**, as well as non-hydroxylated *GeR* and **6-ROX** (**13c**), conjugated to HaloTag(O2) amine ligand. For labeling of tubulin filaments, HeLa cells were incubated with noncovalent β -tubulin ligands, prepared from *GeR* and **630GeRH** and *N*-Boc-deprotected docetaxel, connected via 8-amino-octanoic acid linker^[2b] (Figure S1). All dye conjugates mentioned above provided specific staining and good imaging performance in confocal and STED microscopy (Figures S7-S17), with hydroxylated dyes generally requiring higher

concentrations (e.g., 4-5 μM for *630GeRH* instead of 1 μM or below for *GeR*).

Isomerically pure *6-ROX* dye is one of the “big four” dyes (FAM, JOE, TAMRA and ROX) dominating in the dye-terminator DNA sequencing, but has not yet been applied to live-cell imaging. We have demonstrated that the fluorescence of all *6-ROX* dyes (**13a-c**) may be efficiently switched off by de-excitation at 775 nm, making them useful complementary partners in two-color STED nanoscopy with *SiR* or *GeR* labels. Figures 3, S16 and S17 demonstrate that HaloTag(O2) amine conjugate of *575RH* in combination with *GeR*-tubulin or *630GeRH*-tubulin ligand provide high quality two-color images in the most blue-shifted dye pair still applicable for the widely used 775 nm STED laser line.^[17] Comparison of the Figures S9 and S10 confirms that hydroxylation of the rhodamine core in the dye *575RH* improves image quality as related to the commercially available *6-ROX* (Table S1).

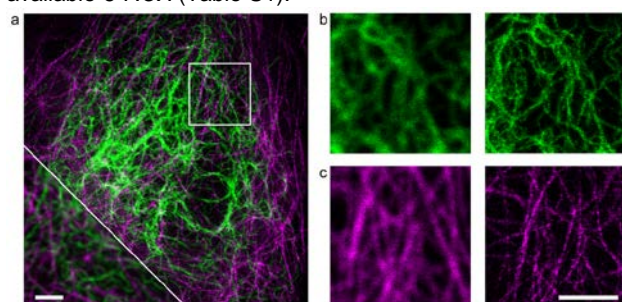


Figure 3. Two-color STED image (raw data) of vimentin-HaloTag fusion protein (green; labeled with 1 μM *575RH-Halo*) and endogenous tubulin (magenta; labeled with 5 μM *GeR*-tubulin) in living HeLa cells, simultaneous incubation time 20 min, followed by 10 min washing. (a) STED image with confocal part in bottom left corner. (b) and (c): zoomed (confocal and STED) views of the region marked in (a) in separate colors. Scale bars 2 μm ; pixel dwell time: 12 μs for both color channels; pixel size: 28 nm for STED and confocal image.

In addition to the labeling of cytoskeleton proteins, the new dyes allow for equally specific staining of nuclear components. Living U2OS and *Drosophila* S2 cells expressing SNAP- and Halo-fusion constructs of different nuclear proteins (TRF2, PML, CID, CAL1) were incubated for 10-30 minutes with 0.5-1.0 μM of the chosen dye combination (*610CP*-BG & *640SiRH*-Halo or *580R*-Halo^[1a] & *640SiRH*-BG; BG = SNAP-tag ligand) resulting in bright staining free from non-specific background (Figure S18). The excellent spectral separation of these combinations allowed for colocalization experiments without spectral unmixing, mapping the nuclear protein interaction with sub-diffraction resolution (Figure S19).

Using the so-called holographic microscopy, we have monitored cell morphology and proliferation of living S2 cells with the constant presence of *580R* and *640SiRH* in the media over 12-16 hours and observed normal cell division (Figure 4) with proper staining of the kinetochore proteins, verified with fluorescence microscopy. Therefore, we conclude that the presence of the protein tags as well as the staining with our dye conjugates does not negatively affect cell viability.

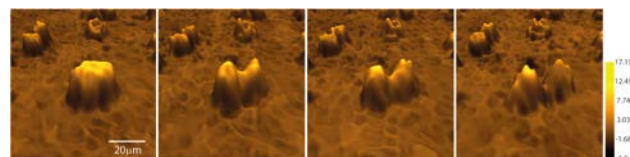
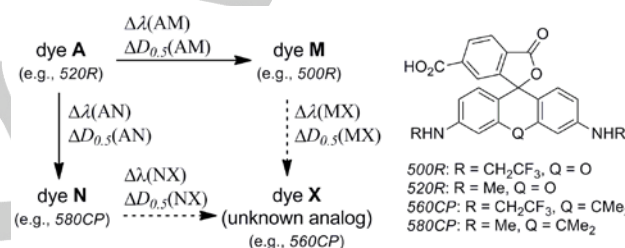


Figure 4. An example of normal cell division (2 min between images) in the presence of *640SiRH* bound to CID-SNAP and *580R* bound to CAL1-Halo after incubation with 0.4 μM *580R*-Halo^[1a] (4 h) followed by addition of 0.4 μM *640SiRH*-BG and imaging for 12 h. Cell viability in the presence of dyes in the centromeres was verified by measuring cell morphology of *Drosophila* S2 cells using a holographic microscope (Holomonitor M4). For the corresponding time-lapse movie, see supplementary Movie.

In view of an expanding palette of live-cell compatible dyes and increasing fluorophore substitution diversity, we propose a general method relying on simple additive schemes to estimate the positions of absorption/emission maxima and $D_{0.5}$ values of the substitution pattern analogs of triarylmethane dyes. For example, using the data of our previous study,^[1a] the properties of dye *560CP* in the same solvent (PBS, pH 7.4) have been accurately predicted before its synthesis (Scheme 3).



Scheme 3. Three reference dyes (A, M, N) are chosen in such a way that M and N differ from the unknown dye X in one structural element. Dye A has one common structural element with dye M, and another common element with dye N. The known changes in properties between A and M (or N) allow estimation of λ and $D_{0.5}$ for X. Assuming $\Delta\lambda(\text{AN}) \approx \Delta\lambda(\text{MX})$ and $\Delta D_{0.5}(\text{AN}) \approx \Delta D_{0.5}(\text{MX})$ (where $\Delta\lambda(\text{AN}) = \lambda(\text{N}) - \lambda(\text{A})$, valid for both absorption and emission maxima; similarly for $\Delta D_{0.5}$), the estimated values for *560CP* are: $\lambda_{\text{abs}}(\text{560CP}) = \lambda_{\text{abs}}(\text{580CP}) + \Delta\lambda_{\text{abs}}(\text{520R}, \text{500R}) = 582 + (500 - 521) \text{ nm} = 561 \text{ nm}$; $D_{0.5}(\text{560CP}) = D_{0.5}(\text{580CP}) + \Delta D_{0.5}(\text{520R}, \text{500R}) = 34.6 + (32.5 - 7.5) = 59.6$. For details, see Figures S20, S21 and Table S2 in the Supporting Information.

In conclusion, the proposed cell- and nucleus-permeant fluorescent dyes allow flexible single- and dual-color labeling in living cells. In STED imaging with de-excitation at 775 nm, several dye pairs have been validated (*575RH* & *635GeRH*, *610CP* & *640SiRH*, and *580R* & *640SiRH*). The improved synthetic approach to silico- and germanorhodamines has been developed, and the new dyes *640SiRH*, *GeR* and *635GeRH* as conjugates with docetaxel offer direct and specific visualization of native tubulin filaments in non-transfected cells. Hydroxylation of fluorophores, especially of lipophilic rhodamines, improves the staining quality at the cost of the necessity to use higher dye loadings. In submicromolar concentrations used for imaging, the dyes of the present study show no evidence of cytotoxicity. The design of future dye analogs can be streamlined with accumulation of photophysical data and estimation of properties of the new candidates using simple additive schemes. The degree of predictive precision achieved by using the measured values for the known structural analogs is higher than the accuracy provided by the present-day computational methods (DFT, TD-DFT), especially for the red-emitting fluorophores.^[18] Further increasing of the spectral and structural variety of cell-permeant fluorophores will

contribute to the design of new experiments in life sciences, including those with more sophisticated multiple color channel separation techniques, such as fluorescence lifetime imaging and hyperspectral detection.

Acknowledgements

We thank J. Bienert (MPIBPC), Dr. H. Frauendorf, Dr. M. John and co-workers (Institut für organische und biomolekulare Chemie, Georg-August-Universität, Göttingen, Germany) for recording spectra; Prof. Z. Novák (Eötvös University, Budapest, Hungary) for the gift of trifluoroethylodinium salt; J. Shimpfhauser and J. Seikowski (MPIBPC) for assistance with the synthesis; Dr. E. Rothermel and T. Gilat (MPIBPC) for the preparation and immunolabeling of cells; Dr. I. Chung, C. Bauer and PD Dr. K. Rippe (Genome Organization and Function, DKFZ) for the U2OS cells used for the nuclear staining and for cloning the TRF2-SNAP and PMLIII-Halo fusion constructs; Dr. A.-L. Pauleau and Prof. S. Erhardt (Zentrum für Molekulare Biologie der Universität Heidelberg, ZMBH) for the *Drosophila* S2 cells stably expressing CID-SNAP and CAL1-Halo fusion proteins; Dr. A. Giske (LEICA Microsystems, Germany) for testing 560CP dye with 660 nm STED laser. S.W.H., A.N.B. and H.S. acknowledge a grant from the Bundesministerium für Bildung und Forschung (FKZ 13N14122). This work was also supported by the Netherlands Organisation for Scientific Research (NWO; grant number 680-50-1501 to R.V.) and EMBO (grant number ALTF 1516-2015 to R.V.).

Keywords: fluorescent dyes • rhodamines • germanorhodamines • optical microscopy • living cells

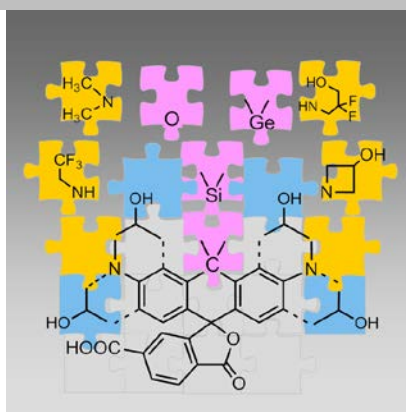
- [1] a) A. N. Butkevich, G. Y. Mitronova, S. C. Sidenstein, J. L. Klocke, D. Kamin, D. N. Meineke, E. D'Este, P. T. Kraemer, J. G. Danzl, V. N. Belov, S. W. Hell, *Angew. Chem. Int. Ed.* **2016**, *55*, 3290–3294; b) F. Bottanelli, E. B. Kromann, E. S. Allgeyer, R. S. Erdmann, S. Wood Baguley, G. Sirinakis, A. Schepartz, D. Baddeley, D. K. Toomre, J. E. Rothman, J. Bewersdorf, *Nat. Commun.* **2016**, *7*, 10778; c) B. Hein, K. I. Willig, C. A. Wurm, V. Westphal, S. Jakobs, S. W. Hell, *Biophys. J.* **2010**, *98*, 158–163; d) S. C. Sidenstein, E. D'Este, M. J. Bohm, J. G. Danzl, V. N. Belov, S. W. Hell, *Sci. Rep.* **2016**, *6*, 26725.
- [2] a) G. Lukinavicius, K. Umezawa, N. Olivier, A. Honigmann, G. Yang, T. Plass, V. Mueller, L. Reymond, I. R. Correa, Jr., Z. G. Luo, C. Schultz, E. A. Lemke, P. Heppenstall, C. Eggeling, S. Manley, K. Johnsson, *Nat. Chem.* **2013**, *5*, 132–139; b) G. Lukinavicius, L. Reymond, E. D'Este, A. Masharina, F. Gottfert, H. Ta, A. Guther, M. Fournier, S. Rizzo, H. Waldmann, C. Blaukopf, C. Sommer, D. W. Gerlich, H. D. Arndt, S. W. Hell, K. Johnsson, *Nat. Methods* **2014**, *11*, 731–733; c) G. Lukinavicius, L. Reymond, K. Umezawa, O. Sallin, E. D'Este, F. Gottfert, H. Ta, S. W. Hell, Y. Urano, K. Johnsson, *J. Am. Chem. Soc.* **2016**, *138*, 9365–9368; d) Y. Kushida, T. Nagano, K. Hanaoka, *Analyst* **2015**, *140*, 685–695.
- [3] L. C. Zanetti-Domingues, C. J. Tynan, D. J. Rolfe, D. T. Clarke, M. Martin-Fernandez, *PLoS One* **2013**, *8*, e74200.
- [4] a) Z. Qian, A. Martyna, R. L. Hard, J. Wang, G. Appiah-Kubi, C. Coss, M. A. Phelps, J. S. Rossman, D. Pei, *Biochemistry* **2016**, *55*, 2601–2612; b) J. P. Richard, K. Melikov, E. Vives, C. Ramos, B. Verbeure, M. J. Gait, L. V. Chernomordik, B. Lebleu, *J. Biol. Chem.* **2003**, *278*, 585–590; c) M. Silhol, M. Tyagi, M. Giacca, B. Lebleu, E. Vives, *Eur. J. Biochem.* **2002**, *269*, 494–501.
- [5] K. W. Teng, Y. Ishitsuka, P. Ren, Y. Youn, X. Deng, P. Ge, A. S. Belmont, P. R. Selvin, *eLife* **2016**, *5*, e20378.
- [6] J. B. Grimm, B. P. English, J. Chen, J. P. Slaughter, Z. Zhang, A. Revyakina, R. Patel, J. J. Macklin, D. Normanno, R. H. Singer, T. Lionnet, L. D. Lavis, *Nat. Methods* **2015**, *12*, 244–250.
- [7] M. J. Hinner, K. Johnsson, *Curr. Opin. Biotechnol.* **2010**, *21*, 766–776.
- [8] A. Gautier, A. Juillerat, C. Heinis, I. R. Correa, Jr., M. Kindermann, F. Beaufils, K. Johnsson, *Chem. Biol.* **2008**, *15*, 128–136.
- [9] G. V. Los, L. P. Encell, M. G. McDougall, D. D. Hartzell, N. Karassina, C. Zimprich, M. G. Wood, R. Learish, R. F. Ohana, M. Urh, D. Simpson, J. Mendez, K. Zimmerman, P. Otto, G. Vidugiris, J. Zhu, A. Darzins, D. H. Klaubert, R. F. Buleit, K. V. Wood, *ACS Chem. Biol.* **2008**, *3*, 373–382.
- [10] J. Hanne, F. Gottfert, J. Schimer, M. Anders-Osswein, J. Konvalinka, J. Engelhardt, B. Muller, S. W. Hell, H. G. Krausslich, *ACS Nano* **2016**, *10*, 8215–8222.
- [11] S. Nizamov, M. V. Sednev, M. L. Bossi, E. Heibisch, H. Frauendorf, S. E. Lehnart, V. N. Belov, S. W. Hell, *Chem. Eur. J.* **2016**, *22*, 11631–11642.
- [12] Y. Koide, Y. Urano, K. Hanaoka, T. Terai, T. Nagano, *ACS Chem. Biol.* **2011**, *6*, 600–608.
- [13] For structures of the known Ge-rhodamines (GeR) and Ge-xanthene dyes, see Figure S3 in *Supporting Information* and patents: a) T. Nagano, K. Hanaoka, Y. Koide, T. Egawa, US 20140057312A1; b) J. Braddock-Wilking, T. L. Bandrowski, J. B. Carroll II, US 20150166581; c) T. Nagano, K. Hanaoka, K. Hirabayashi, Y. Yoki, US 20150212073A1; d) W. Zhou, P. Mesenheimer, M. Zhou, US 20140272990A1.
- [14] V. P. Boyarskiy, V. N. Belov, R. Medda, B. Hein, M. Bossi, S. W. Hell, *Chem. Eur. J.* **2008**, *14*, 1784–1792.
- [15] a) T. Egawa, K. Hirabayashi, Y. Koide, C. Kobayashi, N. Takahashi, T. Mineno, T. Terai, T. Ueno, T. Komatsu, Y. Ikegaya, N. Matsuki, T. Nagano, K. Hanaoka, *Angew. Chem. Int. Ed.* **2013**, *52*, 3874–3877; b) T. Egawa, Y. Koide, K. Hanaoka, T. Komatsu, T. Terai, T. Nagano, *Chem. Commun.* **2011**, *47*, 4162–4164; c) K. Hirabayashi, K. Hanaoka, T. Takayanagi, Y. Toki, T. Egawa, M. Kamiya, T. Komatsu, T. Ueno, T. Terai, K. Yoshida, M. Uchiyama, T. Nagano, Y. Urano, *Anal. Chem.* **2015**, *87*, 9061–9069.
- [16] Q. A. Best, N. Sattenapally, D. J. Dyer, C. N. Scott, M. E. McCarroll, *J. Am. Chem. Soc.* **2013**, *135*, 13365–13370.
- [17] Abberior Instruments GmbH offers STED microscopes with the pulsed 595 nm and 775 nm depletion lasers; Leica Microsystems – with 592 nm (gated; CW), 660 nm (gated; CW) and 775 nm (pulsed) depletion lasers; PicoQuant GmbH offers a STED microscope with a 765 nm depletion laser.
- [18] S. Fleming, A. Mills, T. Tuttle, *Beilstein J. Org. Chem.* **2011**, *7*, 432–441.

Entry for the Table of Contents (Please choose one layout)

Layout 1:

FULL PAPER

Modular design for portable dyes: hydroxylated rhodamines, carbopyronines, Si- and Ge-rhodamines absorbing at 530–640 nm showed specific labeling of living cells and provided optical resolution of 50–75 nm in one- and two-color STED microscopy. The established structure-property relationships allow predicting the properties of the new dye analogs.



A. N. Butkevich,* V. N. Belov,* K. Kolmakov, V. V. Sokolov, H. Shojaei, S. C. Sidenstein, D. Kamin, J. Matthias, R. Vlijm, J. Engelhardt and S. W. Hell*

Page No. – Page No.
Hydroxylated fluorescent dyes for live cell labeling: synthesis, spectra and superresolution STED microscopy